Bedform characteristics and biofilm community development interact to modify hyporheic exchange

Sarah Cook[1*], Oliver Price[2], Andrew King[3], Chris Finnegan[2], Roger van Egmond[2], Hendrik Schäfer[3], Jonathan M. Pearson[1], Soroush Abolfathi[1], Gary D. Bending[3]

[1.] School of Engineering, University of Warwick, Coventry CV4 7AL, UK.

[2.] Unilever, Colworth Park, UK.

[3.] School of Life Sciences, University of Warwick, Coventry CV4 7AL, UK.

[*]Author of correspondence: Dr Sarah Cook, School of Engineering, University of Warwick, Library Road, Coventry, CV4 7AL, sarah.cook@warwick.ac.uk

Abstract

The physical and biological attributes of riverine ecosystems interact in a complex manner which can affect the hydrodynamic behaviour of the system. This can alter the mixing characteristics of a river at the sediment-water interface. Research on hyporheic exchange has increased in recent years driven by a greater appreciation for the importance of this dynamic ecotone in connecting and regulating river systems. An understanding of process-based interactions driving hyporheic exchange is still limited, specifically the feedbacks between the physical and biological controlling factors. The interplay between bed morphology and sediment size on biofilm community development and the impact on hyporheic exchange mechanisms, was experimentally considered. Purpose built recirculating flume systems were constructed and three profiles of bedform investigated: i) flat, ii) undulating λ = 1 m ii) undulating λ = 0.2 m, across two different sized sediments (0.5 mm and 5 mm). The influence of biofilm growth and bedform interaction on hyporheic exchange was explored, over time, using discrete repeat injections of fluorescent dye into the flumes. Hyporheic exchange rates were greatest in systems with larger sediment sizes (5 mm) and with more bedforms (undulating λ = 0.2). Sediment size was a dominant control in governing biofilm

growth and hyporheic exchange in systems with limited bedform. In systems where bedform was prevalent, sediment size and biofilm appeared to no longer be a control on exchange due to the physical influence of advective pumping. Here, exchange rates within these environments were more consistent overtime, despite greater microbial growth. As such, bedform has the potential to overcome the rate limiting effects of biotic factors on hyporheic exchange and sediment size on microbial penetration. This has implications for pollutant and nutrient penetration; bedforms increase hydrological connectivity, generating the opportunity to support microbial communities at depth and as such, improve the self-purification ability of river systems.

Keywords: hyporheic exchange, bedform features, biofilm growth, advective pumping, sediment size.

1. Introduction

The hyporheic zone is a transition boundary in which surface water flows into and out of a fixed sediment bed (Sabater & Vila, 1991; Harvey & Wagner, 2000; Clark et al., 2018). Solutes (i.e. pollutants and nutrients) within the hyporheic flow are continuously transferred back and forth across the overlying water column and streambed interface (Boano et al., 2006; Tonina & Buffington, 2007). This vertical bidirectional flow takes place on a relatively small scale, typically centimetres to tens of metres. This distinguishes it from surface flow and the unidirectional flow pathways governing groundwater recharge and discharge (Boano et al., 2006).

Scientific interest in hyporheic flow has gained recent momentum, sustained by an increased appreciation for river connectivity in mediating important ecohydrological processes (Williams & Hynes, 1974; Stanford & Ward, 1993; Gilbert et al., 1994; Battin et al., 2003; 2008; Sawyer et al., 2009; Boano et al., 2014; Huettel et al., 2014; Azizian et al., 2015; Clark

et al., 2018; Schaper et al., 2018). This dynamic ecotone (i.e. meeting point) act as a biogeochemical 'hot spot' creating an interface for the exchange between chemical solutes (Boulton et al., 1998; Gandy et al., 2007) and aquatic biota (Jones and Mulholland, 2000). This, in turn influences ecological community distributions (Boulton, 2007) which drives changes in microlevel processes, including biogeochemical cycling (Triska et al., 1993; Battin et al., 2003; Nogaro et al., 2010; Danczak et al., 2016) nitrogen mineralisation (Krause et al., 2013) and contaminant processing (Stegen et al., 2016). As such, there is a strong coupling between hyporheic exchange and stream functioning, making the hyporheic zone a key focus for river restoration goals (Hester & Doyle, 2008; Magliozzi et al., 2019).

It is well established that hyporheic exchange influences mixing characteristics. This is governed by a range of environmental parameters including: flow rate, sediment composition and channel morphology, particularly bedforms (Marion et al., 2002; Cardenas et al., 2008; Bottacin-Busolin et al., 2009; Boano et al., 2014; Clark et al., 2018). These factors have the capacity to impact the extent to which dissolved pollutants carried in water come into contact with degrader communities and thus, control their environmental fate (Scharper et al., 2018). Increased anthropogenic activity including mining, urban and industrial development, dam construction and agriculture can disrupt the bio-hydrological connections within the hyporheic zone (Hancock et al., 2002). As such, it is vital that a wider understanding of the controls governing hyporheic exchange are investigated. This is necessary if strategies are to be designed that successfully exploit the central role of this ecotone in water quality maintenance.

Undulating bedforms strongly control mixing characteristics by influencing flow resistance and exchange, resulting in flow separation and associated energy dissipation (Wijbenga, 1990; Ogink, 1988; Julien et al., 2002). Research has demonstrated that the larger the

amplitude (i.e. height) of the bedform the greater its impact on hydrological exchange (Elliott and Brooks, 1997; Marion et al., 2002; Packman et al., 2002). Solutes, both pollutants and nutrients, within the flow have the potential to penetrate to deeper depths in bedforms with smaller wavelengths and increase the hydrological connectivity of the riverbed. This facilitates deeper nutrient and pollutant distribution as well as altering environmental conditions. However, microbial community growth, alongside the flow through undulating bedforms and the hydrological connectivity between bedforms of different wavelengths is poorly understood in a river system. Central to this is the concept of 'pumping' whereby differences in bed topography create pressure and flow gradient variations across the river bed (O'Connor & Harvey, 2008). Bedform impediments can create high-pressure regions upstream of the obstruction and low-pressure regions downstream. This differential pressure can drive the overlying water into the interstitial pore spaces creating flow pathways through the obstruction and hyporheic circulation underneath (Tonina & Buffington, 2007). This can, in turn, alter the rate of hyporheic water mixing within the channel (O'Connor & Harvey, 2008).

Microorganisms grow and also excrete extracellular polysaccharides, enabling them to cover the riverbed, forming a biofilm (Wimpenny et al., 2000). These colonizing microbes, particularly prokaryotes and algae, alongside fungi and protozoa in mature biofilm, drive biogeochemical cycling processes (Fischer et al., 2005) as well as immobilising and dissipating contaminants and pollutants through sorption and degradation (Jarvie et al., 2005). The importance of these microbial communities in lotic ecosystems has been widely recognised (Battin et al., 2016). Previous research has identified how bedform amplitude impacts both hyporheic exchange and solute residence times (Elliott & Brooks,1997; Marion et al., 2002; Packman et al., 2002; Tonina & Buffington, 2007; O'Connor & Harvey, 2008;

Aubeneau et al., 2016). However, there is a need to determine how bedform morphology (i.e. amplitude and wavelength) influences biofilm formation and the feedback on hyporheic exchange, which remains largely unknown.

Changes in the water-sediment exchange can interact with and modify water flow patterns (Nogaro et al., 2013; Battin et al., 2016). For example, previous research has demonstrated a reduction in interstitial water flow around benthic biofilms (Bottacin-Busolin et al., 2009; Orr et al., 2009; Larned et al., 2011), resulting in alterations in solute residence time distributions (Aubeneau et al., 2016). In addition, the growth of these benthic biofilms on sediments clogs the interstitial pore spaces within the sediment layers (Battin et al., 2008; Aubeneau et al., 2016). This can alter the hydraulic conductivity of the sediment, impeding water penetration and solute transfer within the hyporheic zone (Nogaro et al., 2010; Aubeneau et al., 2016).

In-situ studies have observed variability in biofilm growth in accordance with sediment composition, specifically particle size (Nogaro et al., 2010). Aubeneau et al. (2014) noted a 25% greater exchange rate in channels with coarse gravel particles (5 cm) versus those with finer sediment (0.5 cm). This is partly attributed to the smaller infiltration capacity of finer sediments. As such, nutrient penetration is reduced, restricting the layer and depth of surface biofilm growth (O'Connor & Harvey, 2008).

There have been a number of studies that have examined how the physical attributes (i.e. submerged bedform) of a habitat influence hyporheic fluxes (Magliozzi et al., 2018). This has been achieved through simulations (Elliott & Brooks, 1997; Boano et al., 2014), laboratory experiments (Tonina & Buffington, 2007; Haggerty et al., 2014) and *in-situ* field studies (Zimmer and Lautz., 2014; Lautz & Bauer, 2006). Similarly, the effect of the hyporheic exchange on the microbial community has been investigated (Nogaro et al., 2013; Caruso et

al., 2017). However, few studies have studied the mutual impact and interactions of bed morphology and biofilm on the hyporheic zone exchange (e.g. Bottacin-Busolin et al. 2014). As such, a mechanistic understanding of how hyporheic exchange is regulated and controlled is underdeveloped due to the complexity of natural systems.

Here, we present an innovative approach to examine how bedform features such as dune wavelength and sediment size can interact with biofilm communities at both i) the sediment-water interface and ii) bed profile depth, using an experimental flume system. Using fluorescent dye tracer experiments we then examine how this feeds back on hyporheic exchange and discuss the role of pumping in driving both biofilm growth and feedbacks on fluvial mixing. To our knowledge, the work presented here is the first attempt to explicitly consider the entire bed profile (i.e. sediment size, bedform, dune wavelength) in assessing both the physical and biological impacts on hyporheic exchange. This is of functional importance for environmental remediation and restoration strategies, with functioning streambed interfaces also aiding in wider catchment nutrient cycling and maintenance of healthy streambed communities.

2. Methods

2.1 Water extraction site

Water employed in the flumes was taken from the River Dene, a minor tributary of the River Avon, Warwickshire UK, which flows approximately 16 km from its origin in Burton Dasset Hills near Kineton to its confluence near Charlecote Park. The River Dene is surrounded by a mixture of land use; nearby urban transport routes, residential and commercial areas, but is predominantly agricultural. River water (pH 7.3; Phosphate levels 21 μg ml^{-1} Nitrate 26 μg

ml^{-1}) was collected from Wellesbourne (52°11'51.7"N 1°36'09.3"W) and was first passed through a 200 μm mesh and then a 38 μm mesh to remove particulate matter. The water was then transferred to the flumes within 2 hours of initial collection.

2.2 Flume design

A custom-built recirculating flume experimental system was constructed enabling tracer studies to be conducted in a replicate system with identical physical and hydraulic characteristics. The experimental system consisted of 9 recirculating rectangular flume channels, comprised of 3 separate units each containing 3 flumes. Each flume was 1.98 m long, 0.1 m wide and 0.2 m deep (Figure 1). The flumes were constructed from 0.01 m thick glass allowing for a clear visual observation of the experiment. To maintain the structural rigidity of the system an aluminium frame was constructed to hold the flumes in place. The frame had adjustable legs which aided in generating sufficient flow depth along the channel length for different bedform morphologies. The slopes placed on the flumes created a gravity chute down which water could flow. The water flowed over a weir, positioned downstream, which could be adjusted accordingly to achieve uniform flow. The water then proceeded down a pipe and through a flow meter where a Grundfos UPS15 recirculating pump then pumped the water through additional piping back into the flume system (Figure 1). Average flow depth and bed height was fixed at 0.03 m and 0.1 m respectively, with a discharge of 12 L min^{-1} to ensure sufficient water mixing.

2.3 Range of experimental flow conditions

In the experiments we systematically varied bed-profiles. Experiments were run over a maximum of 20 days with data collected every 2 days. Three profiles were chosen: i) flat, ii) undulating with two dunes (λ = 1 m), iii) undulating with multiple dunes (λ = 0.2 m) (Figure 2a). Two sizes of smooth synthetic glass beads (VWR International) were applied for each of the bedding profiles. The glass beads may have affected the penetrance of light into the sediment and thus, permitted greater biofilm depth penetration. However, the choice to use glass beads minimised sorption as a factor, as the synthetic glass beads were smooth and impermeable, adding uniformity to the bed sediment. The mean particle sizes chosen for investigation were 5 mm and 0.5 mm to represent gravel and coarse sand environmental conditions, respectively. In summary a total of six bedding profiles were investigated.

Each set of bed profiles was allocated its own bank of three flumes enabling each experiment to be run in triplicate. Experiments were first conducted using the 0.5 mm particle size, after which the flumes were cleaned with ethanol before bed profiles were created with the 5 mm particle size.

The artificial substrates were poured into the bed section of the recirculating flume to an average bed height of 0.1 m, with a maximum dune height of 0.11 m from peak to base (Figure 2a). Templates were constructed for each of the bed profiles and sediment weight used in each system was logged.

2.4 Analytical method to determine hyporheic exchange

Hyporheic exchange in natural systems is controlled by a complex array of both biological, chemical and physical processes. It can be modelled using an effective dispersion coefficient (*D)* which encompasses these complex interactions and can be formulaically displayed as,

$$D = \beta\ (D_m + D_b) + D_d \qquad (1)$$

where: β is the sediment diffusion correction term, D_b is the biodiffusivity ($L^2\ t^{-1}$; i.e. biologically mediated diffusive transport of solutes and solids in sediments), D_d is the dispersion coefficient (encompassing turbulent diffusion and pumping, $L^2\ t^{-1}$) and D_m is the molecular diffusion coefficient ($L^2\ t^{-1}$), all of which can be obtained empirically or through modelling (Berg et al., 1998).

O'Connor & Harvey (2008) developed a succession of scaling relationships that related effective diffusion coefficients to a variety of fluid flow and sediment characteristics, a concept originally proposed by Richardson & Parr (1988). A measured value of effective diffusion over a sediment can be determined indirectly using a conservative tracer (e.g. Rhodamine) in a closed system (i.e. laboratory flume). In this case the concentration (C) is initially 0 in the bed sediment. The concentration in the overlying water column (C_{wc}) is equal to an initial concentration (C_0). As the water recirculates, hyporheic exchange will drive the tracer into the sediment interstitial pore space resulting in a decrease in concentration in C_{wc} over time. As such, the slope of a temporal concentration profile (i.e. C_{wc} versus $t^{1/2}$) can be used to calculate D, briefly

$$D = \left(\frac{\sqrt{\pi}}{2}\frac{V_w}{A_s}\frac{dC^*}{d(t^{1/2})}\right)^2 \qquad (2)$$

Where: V_w is the volume of the overlying water column in the recirculating flume (m^3), A_s is the surface area of bed sediment (m^3), C^* is the normalised solute concentration (i.e. C_{wc} / C_0)

Fluorescent tracing was used to quantify the rate of solute penetration at the water-sediment interface. Rhodamine was chosen as the tracer due to its high detectability and low levels of photochemical decay. Turner Design Cyclops 7 fluorimeters were used to measure the change in tracer fluorescence (as a voltage output) in the channel over time. These were placed in the inlet of the flume so that decreases in fluorophore levels in the water column (an indication of hyporheic exchange within the interstitial sediment pore space) could be monitored (Figure 1).

The Rhodamine tracer was introduced into the centre of the channel at the outlet weir. The solute was made up to a concentration of 10^6 ppb which was diluted using water extracted from the flume. The amount of injected Rhodamine was designed to increase fluorescence level to 30 ppb by the time equilibrium had been reached. The equilibrium states of each experiment was assumed when the sediment transport rate and bed height were invariant. To determine this Vernier depth gauges were placed along the length of the channels. The bed height and water depth were measured in relation to the flume base at two points, across the width, every 0.1 m along the length of the flume. After the achievement of equilibrium the sediments were assumed to remain constant, with bed morphology remaining constant throughout the experiment. Repeat discrete injections of tracer were added into each flume at 48-hour intervals.. After data collection the voltage data was converted into a concentration (ppb). Voltage and concentration were related by a linear relationship obtained by calibration.

2.5 Biofilm growth

Biofilm growth was measured i) temporally on the sediment surface every 48 hours for 20 days and ii) within the bed profile (i.e. every 1 cm in 10 cm depth) after 20 days. The flume units were placed in a controlled environment room, light was used to stimulate the photosynthetic growth of algae and cyanobacteria, and therefore accelerate biofilm growth within the interstitial pore spaces. Fluorescent daylight bulbs were covered with Lee DS 226 UV filter screens to prevent transmission of light wavelengths < 380 nm. The lights were set on a timer to provide 16 hours of light and 8 hours of dark. The collected river water acted as an inoculum to permit microbial growth in the system.

Modifications to the experimental design were made to permit the quantification of *in-situ* microbial growth within each unit (Figure 2b). This included the addition of 2.5 cm^2 length glass sides on the surface to act an extractable synthetic surface (Kowalczyk et al., 2013) from which to extract and quantify surface biofilm (Figure 2b). The slides were placed in triplicate along the length of the flume starting at t = 0, spaced at 20 cm intervals along the sediment bed. During the experiment three slides were extracted every 48 hours from the same locations on each experimental unit to asses biofilm growth rate on the surface of the sediment bed. Biofilm was resuspended and carbohydrate was quantified using a phenol-H_2SO_4 assay (Kowalczyk et al. 2016, and further described in Dubois et al. 1959) as a proxy for biomass.

The sediment bed was also cored in order to quantify biomass growth within the bed profile at depth. Due to the destructive sampling involved, coring was only undertaken at the end of the tracer experiment (i.e. after 20 days, to a depth of 10 cm). Sediment cores were taken every 20 cm (Figure 2b), in triplicate, along the sediment bed using perspex corers (length 10 cm; diameter 2 cm). Once removed the cores were frozen and dissected into sections of 1 cm

intervals using a scalpel. Each 1 cm segment was placed into a 25 ml Falcon tube with 5 ml of water and vortexed to suspend the biofilm. Following biofilm extraction, the biofilm biomass was analysed for carbohydrate content in the same manner as described above.

2.6 Statistical analysis

2.6.1 Biofilm growth

We applied a multiple linear regression (MLR) approach to test whether sediment size (two levels factor: 5 mm and 0.5 mm, explanatory variable) and bedform type (three level factor: flat, two-dune, multi-dune, explanatory variable), control the biofilm biomass (response variable, number of samples (n) = 540) within the bed sediment at the final timepoint (20 days). Subsequently, we also tested under the same approach the effect of sediment size (explanatory variable) and bedform type (explanatory variable) on the surface biofilm biomass over time (response variable, n = 198). In this instance, we also included time (continuous covariant) in the model as a controlling variable for the non-independence of the repeated observations over time.

The generated MLR model coefficients were used to calculate the modelled relationship between factors and compared to the observed values. All output results from the regression models are provided in the Supplementary Material (Tables S1-S2; Figure S3), alongside the model metric outcomes (standardized beta values, t statistic = t, degrees of freedom = df, adjusted r^2 and p value) and the number of samples (N).

2.6.2 Hyporheic exchange

The initial slope of the concentration profile (i.e. C_{wc} versus $t^{1/2}$) referred to hereafter as the 'exchange gradient' was used as a metric of hyporheic exchange. We selected biofilm, sediment size and bedform as the likely controlling factors governing the hyporheic exchange. A MLR model was applied to the dataset to produce a unique model integrating biofilm biomass (explanatory variable), sediment size (explanatory variable) and bedform (explanatory variable) as predictors for hyporheic exchange (response variable; n = 198; Table S3, Supplementary Material). Linear regression was also used to test observed trends between hyporheic exchange and biomass across experimental systems. All output results from the regression models are provided in the Supplementary Material (Tables S3; Figures S4-S5), alongside the model metric outcomes (standardized beta values, t statistic = t, degrees of freedom = df, adjusted r^2 and p value) and the number of samples (N).

The performance of all the models were assessed using the following metrics:

a) The coefficient of determination (R^2) for the regression between measured and modelled biofilm amounts/ hyporheic exchange.
b) The Nash-Sutcliffe efficiency (Nash and Sutcliffe, 1970), a measure of goodness of fit between the modelled and measured data i.e.:

$$NSE = 1 - \frac{\sum(measured - modelled)^2}{\sum(measured - mean)^2} \quad (3)$$

where '*measured'* is the measured data, '*modelled'* is the modelled amount estimated using the various predictors and '*mean'* is the mean measured data. The closer the NSE is to 1 the

stronger the model fit. A value of 0 or lower indicates that the model performs no better than the mean of the data (Nash and Sutcliffe, 1970).

Statistical analysis (including: descriptive statistics, alongside multi-linear and linear regression) was performed using Graphpad Prism v8 (GraphPad Software, Inc., www.graphpad.com) and SPSS v25 (SPSS Inc., Chicago, Ill., USA). The threshold for statistical significance was set at a confidence level of 95% but greater significance was noted. Normality and homogeneity of variance was tested on the residuals using the Shapiro-Wilk test and Levene's tests, repectively.

3. Results

3.1 Biofilm growth

Microbial growth was measured on the surface and at depth across all experiment flume systems (Figure 3 to 6). Biofilm growth gradually increased over the course of all experiments (Figure 3) and was concentrated on the sediment surfaces, irrespective of sediment size or bedform (Figure 4 to 6).

The maximum biofilm biomass was 105.1 ± 6.1 and 115.1 ± 6.0 μg carbohydrate equivalent mm^{-3}, respectively for the 5 mm and 0.5 mm sized particles, within the flat bed system, stabilising around day 10. The two-dune (λ = 1 m) system reached peak biofilm growth, across both particle sizes, by approximately day 10 (Figure 3) at which peak biofilm growth plateaued. Biofilm growth was slower within the multiple-dune system (λ = 0.2 m) across both sediment sizes but reached the highest levels from day 12 (Figure 3). Biomass reached a

peak of 129.1 ± 6.4 and 106.1 ± 5.8 μg carbohydrate equivalent mm^{-3}, respectively for the 5 mm and 0.5 mm sized particles for the two-dune system and 131.2 ± 7.2 and 149.4 ± 8.7 μg carbohydrate equivalent mm^{-3} within the multi dune system.

A MLR analysis between bedform and sediment size (explanatory variables) and day (controlling factor) revealed all three parameters were significant (adjusted r^2 = 0.76) in predicting changes in biomass over time (bedform, t = 2.21, p<0.0001; days, t = 24.13, p<0.0001; sediment size, t= -6.43, p<0.0001; degrees of freedom, df = 194).

After 20 days there was a trend for higher levels of surface biofilm growth on the 0.5 mm compared to the 5 mm sediment particle size across all systems, and biomass reduced with depth across all experimental systems (Figure 4 to 6). In the flat bed system there was a gradual reduction within the 5 mm sediment systems, with only a 40% reduction in biomass at a depth of 6 cm (Figure 4). Conversely, the 0.5 mm sediment systems displayed a rapid reduction in biomass with depth, with a 42% reduction in biomass observed after a depth of only 2 cm (Figure 4). By contrast, two-dune system generally did not exhibit sudden drops in the maximum biofilm growth until approximately 3 cm in depth (Figure 5), with biomass levels in the multi-dune beds typically only dropping rapidly after a depth of around 4 cm (Figure 6). Biofilm depth infiltration extent varied depending on the dune sample location from where the core was extracted (i.e. up-slope, slope peak etc; Figures 5 and 6). The MLR model revealed that depth (t= -32.46, p< 0.0001), sediment (t=7.93, p<0.0001) and bedform (t = 4.32, p <0.0001, df = 536) were the dominant controlling factors governing biofilm growth (adjusted r^2 = 0.68), within the bed profile (Table S2, Supplementary Material).

Using the generated model coefficients (Tables S1-2, Supplementary Material) biofilm biomass was plotted as a function of sediment size and bedform across time (Figure 7a) and

with depth (Figure 7b). As expected, both the modelled and measured data displayed a significant correlation between biofilm biomass growth over time (Figure 7a) and with depth (Figure 7b), across all sediment sizes. Days explained 71% to 79% of the biofilm data across the 0.5 mm and 5 mm sediment systems (Figure 7 a), respectively, with depth having a greater control in biomass growth within the 5 mm sediment systems, explaining over 70% of the biofilm data, in contrast to 64% in the 0.5 mm sediment systems (Figure 7b). Both modelled temporal and depth biomass data correlated strongly to the measured data producing r^2 values of 0.76 and 0.68, respectively (Table 1; Figure S3; Supplementary Material). This corresponded to NSE metrics of 0.74 and 0.90 for the depth and temporal data sets, respectively (Table 1).

3.2 Hyporheic exchange

To elucidate whether the growth of microbial communities on the flume bedforms impacted hyporheic exchange, the trace data was normalised to permit the identification of temporal changes in exchange gradients. A MLR analysis and model was constructed using sediment size, bedform and biomass as predictors for hyporheic exchange over time. The MLR analysis releveled that 70% of the variance in hyporheic exchange was controlled by a combination of these three factors. Using the model coefficients hyporheic exchange was modelled across all experimental systems. There was a weak but significant correlation between the modelled and measured hyporheic exchange data (Table 1; Figure S4, Supplementary Material). However, the low overall NSE metric, 0.38, suggested a poor overall fit between the modelled and measured hyporheic exchange data, using sediment size, bedform and biomass as predictors.

A linear regression between biomass and hyporheic exchange (Figure 8a) revealed there was a strong correlation between these two parameters within the two dune (r^2 = 0.60, p<0.0001, df = 31) and flat dune (r^2 = 0.45, p <0.0001, df =31) 0.5 mm sediment systems, with no significant relationship between biofilm and hyporheic exchange reported in any of the 5 mm sediment systems (Figure 8b). Here, increased bedform complexity resulted in a larger hyporheic exchange, regardless of the biofilm present. This trend is emulated within the multi dune 0.5 mm sediment system, which also displayed consistently higher hyporheic exchange gradients than the flat or two dune systems when biomass was below 75 μg mm^{-3} (Figure 8a). A predictive model for hyporheic exchange, within the flat and two-dune 0.5 mm sediment systems, was built using biofilm alone (Table 1; Figure S4, Supplementary Material). This revealed a moderate goodness of fit (r^2 = 0.54; p <0.0001; df = 64, NSE 0.60) between the measured and modelled hyporheic exchange data sets.

4. Discussion

4.1 Surface biofilm growth

Utilising river water as inoculum in the experimental systems provided an insight into the process of microbial community growth in sediment beds. All flume systems permitted the growth of microbial communities both on and within the sediment beds. Biofilm succession greatly varies on artificial substrates, with algal colonisation divided up into three components: i) green algae, ii) diatoms and iii) cyanobacteria (Sekar et al., 2004). However, the pattern of succession can be highly dependent on river ecosystem and differences in water quality. (Tien et al., 2009; Li et al., 2017; Cai et al., 2018). Bedform and sediment size were all significant in controlling the surface biofilm growth, that significantly increase over time, and were good model predictors. Battin et al. (2016) noted large changes in sediment surface area associated with different sediment particle sizes. For example, one cubic meter of

homogenous sediment with a particle size of 5 cm and 0.5 cm have a corresponding surface area of 100 m^2 and 1000 m^2, respectively. Our observations are consistent with those proposed by Battin et al. (2016) with the small particle size beds creating a greater sediment surface area and total area for microbial colonization. This could also help to promote a greater biogeochemical exchange (Parker et al. 2018) driving higher biofilm community metabolism and thus, promote microbial growth further. Biofilm growth was slower within the multiple dune systems but reached higher peaks across both sediment sizes, in comparison to the flat and two-dune systems.

In river systems this localised development of organic matter (i.e. biofilms), can impact sediment hydraulic conductivity and permeability, reducing rates, and in turn, increase residence times across the hyporheic zone (Gomez-Velez et al., 2015; Peralta-Maraver et al., 2018). These biofilms act as 'hyporheic bioreactors' (Peralta-Maraver et al., 2019) with the operational metabolic capacity to degrade and consume a wide range of compounds. This, combined with longer residence times has the potential to improve downstream water quality through the removal of contaminants and enhanced river connectivity (Peter et al., 2019). However, Harvey et al., (2013) demonstrate that to achieve this there must be a balanced ratio between hyporheic residence to reaction time. Otherwise an imbalance will cause the reactants to be used up promoting the storage of biochemically inactive water (Harvey et al., 2019).

4.2 Biofilm growth with depth

In general, higher amounts of biofilm developed on the smaller experimental substrate (0.5 mm) and was concentrated on the surface of the bedform. There was a reduction in microbial community biomass with depth in all flume systems irrespective of sediment size and bedform, a trend demonstrated by several researchers (e.g. Nogaro et al., 2013; Danczak et

al., 2016). However, in general, the 5 mm particle size permitted greater autotrophic biofilm depth penetration across all bedforms. This trend is supported by observations from several *in-situ* based river studies (Nogaro et al. 2010; Parker et al. 2018). Depth, particle size and bedform were strong predictors for biofilm growth in the sediment bed. This is likely attributable to porosity which is known to influence the exchange of flows and energy in fluvial systems (Sawyer & Cardenas, 2009; Nogaro et al., 2010). The larger pore spaces within the 5 mm system will permit more water and light to penetrate the entirety of the sediment bed, as well as maintain aerobic conditions (Elliott & Brooks, 1997), which could also contribute to a more intensive exchange of matter. As such, the porous structure may allow the biofilm matrix to spread deeper into the sediment bed (Packman et al., 2004) as well as encourage interstitial habitat colonisation.

By the same logic the restricted interstitial pore space in the 0.5 mm sediment systems will inhibit effective diffusion into the sediment bed, confining nutrients and biofilm growth to the sediment surface layers (Nogaro et al., 2010). This is reflected in the rapid reduction in surface biomass, for all 0.5 mm particle size test studies, in response to sediment core depth. The feedback from microbial growth will promote rapid bioclogging of the interstitial pore spaces creating impermeable bedforms. This feature has been shown to alter flow dynamics with Haggerty et al. (2014) reporting an increase in transient storage times by a factor of 4 in response to biofilm clogging.

Greater biofilm depth penetration was observed in the systems with a greater number of dunes. This is particularly evident when comparing the 0.5 mm sediment systems. Biomass dropped immediately after only a depth of 1 cm within the flat bed system. By contrast, two-dune system generally did not exhibit sudden drops in the maximum biofilm growth until approximately 3 cm in depth, with biomass levels in the multi-dune beds typically only

dropping rapidly after a depth of around 4 cm. The presence of dunes increases hydraulic roughness by protruding into the flow (Paarlberg et al. 2009). High pressure regions develop upstream of the obstruction with low pressure forming downstream, creating a pressure gradient, which pumps through the obstruction and increases flow connectivity (Tonina & Buffington, 2007). As such, the greater number of bedforms within the dune systems may be creating a strong pumping mechanism, permitting nutrients to be propelled further into the sediment bed, supporting biofilm growth. This could also explain why biofilm growth on the sediment surface was slower within the multi-dune systems.

Pumping may be enabling the biofilm matrix to overcome the physical constraints of the 0.5 mm sediment. As such, biofilm is likely controlled by the light and nutrient deficit experienced with increased sediment depth. This could explain why biomass levels tended to be greater on the up and peak slope locations within the multi-dune and two-dune systems, where the force of pumping is likely greater. Equally, the lower pressure experienced after the dune structure would explain why the down-slope and trough sections tended to exhibit lower biomass concentrations with increasing sediment depth. From an ecological perspective, these biological drivers emphasise the importance of considering not only the magnitude of the hyporheic exchange flux but also the flow pathways within the hyporheic zone, which play an equally crucial role in modulating biogeochemical river processes (Lewandowski et al., 2019).

4.3 Hyporheic exchange mediating factors

Impact of microbial growth on the hyporheic exchange was quantified by repeat discrete dye injections into the flume systems. Hyporheic exchange was controlled by a combination of sediment size, bedform and biofilm, with sediment size the dominant controlling factor. This is visually supported by the faster rate of exchange in systems with a larger sediment particle size (i.e. 5 mm) and in systems with bedforms present. These findings are in-keeping with the

theoretical background regarding sediment size and bedform structures (Elliott and Brookes, 1997; O'Connor and Harvey, 2008; Magliozzi et al. 2018). Within the 0.5 mm sediment systems biofilm was the dominant controlling factor, and predictor, of hyporheic exchange within flat and two dune environments. In these sediment systems, exchange gradients became progressively slower with increased biofilm. This implies that the microbial growth and associated bioclogging, over time, impeded the rate of hyporheic exchange. This is reinforced by Aubeneau et al. (2016) noting decreases in conservative solute transport in response to biofilm growth.

Conversely, the multi-dune system exhibited the opposite trend to the 0.5 mm sediment flat and two-dune systems with no significant change in exchange rates identified in relation to biofilm growth. This implies that microbial growth had limited impact on the movement of water through the sediment, despite increased biofilm overtime. Similarly, exchange rates were consistent across all 5 mm sediment experimental series, despite changes in biofilm growth. This suggests that the 5 mm sediments used in the test system are too large to permit sufficient quantities of microbial growth on the surface to impede effective diffusion. This is supported by greater biofilm growth at depth within the 5 mm particle systems. This could also explain why the model to predict hyporheic exchange as a function of biofilm, sediment size and bedform performed poorly within the 0.5 mm multi-dune system and all 5 mm experimental systems. The integration of more intermediate sediment sizes within the experimental framework would help in modelling the predictive forces of bedform and sediment size in response to hyporheic exchange.

Here, bedform was identified as the major controlling factor determining exchange rates, with a greater number of dunes contributing to higher rates of hyporheic exchange. This, coupled with the consistent levels of exchange reported in the multi-dune 0.5 mm sediment

system adds support to the concept of pumping. Pumping will become 'activated' from the increased presence of bedforms, reflected in more consistent and higher exchange rates in the multi-dune system, irrespective of sediment size. This mechanism was sufficient to force the Rhodamine tracer through fine particles and thus, overcome the i) small interstitial pore spaces and ii) excess clogging of the small interstitial pore spaces overtime. Greater advective mass transfer between the water column and stable sediment bed will create a positive cascade effect within the system. Faster water exchange will shorten residence times and lower microbial growth. This is supported by the slower biofilm growth rates within the multi-dune system. This will, in turn, reduce interstitial pore space clogging and further increase the rate of exchange between the water and sediment column. In a river environment these mechanisms can work to increase material transport (e.g. pollutants; Peralta-Maraver et al., 2019) and water influx into the sediment. Enhanced vertical flow could aid in the removal of trace organic compounds, by increasing contact between microbial degraders and the pollutant (e.g. pharmaceuticals; Schaper et al., 2019). However, this increased contact can simultaneously permit the input of substances into the hyporheic zone (Peralta-Maraver et al., 2019) should the microbial potential for biodegradation be absent. This can have implications for chemical persistence allowing greater mobility and deeper sediment penetration with potential groundwater contamination (Liu et al., 2019).

It is commonly recognised that hyporheic flow depends on high and low permeability regions within the stream bed (Sawyer et al., 2009; Packman et al., 2002). Laboratory recirculating flume experiments have identified differences in the flow pathways over permeable versus impermeable beds of the same topography (Cooper et al., 2017). In general, turbulence over permeable beds is less intense resulting in greater energy flow and momentum transport. The force generated from pumping enhances the permeability potential of the sediment. As such,

energy levels within the dune environments will likely be higher further contributing to higher rates of material transport across the sediment-water interface.

However, it is also important to note that biofilm growth is cyclically associated with changes to morphology and physiological states (Hall-Stoodley & Stoodley, 2002) and can result in microbial community detachment from the sediment (Chen et al., 2017). This could explain why peak exchange rates within the multi-dune 5 mm system are observed (i.e. -0.0091) alongside times of peak surface biofilm (i.e. 112 μg mm^{-3}), as the interstitial pore spaces became unclogged, thus increasing hyporheic exchange. The larger pore space may also encourage unclogging. As such, hyporheic exchange could be dependent upon biofilm stability; if microbial communities develop to the point at which sloughing occurs (detachment of portions biofilm), any inhibition on exchange can potentially be reversed.

This study uses biomass as a surrogate for total biofilm growth, ignoring the structural and functional taxonomic diversity that makes up the biofilm matrix. This paper identifies a potential reciprocal interaction of hydrodynamics within the physical structure and biofilm growth in the pore space. This interaction could have significant repercussion on the biotransformation of pollutants and nutrient recycling. Research by Scheidweiler et al. (2003) explores this further, providing evidence that biofilms are able to differentiate and actively remodel their matrix, in porous environments, in order to exploit their surrounding space. This can increase their carrying capacity and function as hyporheic bioreactors. This is further supported by Battin et al. (2003) noting the functional ability of biofilms to increase hydrodynamic transient storage of stream water and retention of suspended particles, feeding back into biochemical process changes. Subsequently, further analysis into the succession of biofilms both over time and depth would make a natural extension to the current investigation. Furthermore, given the impact of bedform and its link with advective pumping,

further investigations should seek to explore how bedform height also impacts hyporheic exchange.

5. Conclusion

This research highlights the important and interconnected feedback mechanisms involved in both driving and sustaining water-sediment interactions. Biological changes in the flume systems exerted a strong control on the conservative transport of our solute, supported by the fact that no modifications were made to the flume systems during each experiment series and microbial communities were freely allowed to proliferate. The extent of biological control was strongly influenced by the environment's physical parameters including bedform structure and particle size. These physical controls, in turn, feedback into the biological system and can work to dampen or intensify the biological influence on solute transport. Bedform structures have the potential to overcome the flow limited effects of biofilm clogging which is enhanced in systems with larger sediment sizes. This finding is of functional importance for both river management and stream restoration design but also water quality. More bedform features and greater hyporheic exchange rates could aid in driving water purification, nutrient recycling and altering streambed community organisation. As such, understanding more about the coupling between microbial and hyporheic flow represents an important frontier of research for ecosystem scientists.

Acknowledgments

We are grateful for the funding provided by both the Natural Environmental Research Council (Grants NE/H018980/1 and NE/R003645/1) and Unilever. We also thank three anonymous reviewers for taking the time to thoroughly read our manuscript and provide constructive feedback for its improvement.

References

Aubeneau, A.F., Hanrahan, B., Bolster, D. and Tank, J. 2016. Biofilm growth in gravel bed streams controls solute residence time distributions. Journal of Geophysical Research: Biogeosciences 121, 1840-1850.

Aubeneau, A.F., Hanrahan, B., Bolster, D. and Tank, J.L. 2014. Substrate size and heterogeneity control anomalous transport in small streams. Geophysical Research Letters 41, 8335-8341.

Battin, T.J., Besemer, K., Bengtsson, M.M., Romani, A.M. and Packmann, A.I. 2016. The ecology and biogeochemistry of stream biofilms. Nature Reviews Microbiology 14, 251 – 263.

Battin, T.J., Kaplan, L.A., Findlay, S., Hopkinson, C.S., Marti, E., Packman, A.I., Newbold, J.D. and Sabater, F. 2008. Biophysical controls on organic carbon fluxes in fluvial networks. Nature Geoscience 1(2), 95-100.

Battin, T.J., Kaplan, L.A., Newbold, J.D. and Hansen, C.M. 2003. Contributions of microbial biofilms to ecosystem processes in stream mesocosms. Nature 426, 439-442.

Berg, P., Risgaard-Petersen, N. and Rysgaard, S. 2003. Interpretation of measured concentration profiles and sediment pore water. Limnology and Oceanography 43, 1500-1510.

Boano , F., Camporeale , C., Revelli , R. and Ridolfi, L. 2006. Sinuosity-driven hyporheic exchange in meandering rivers. Geophysical Research Letters, L18406.

Boano , F., Harvey , J.W. Marion , A., Packman , A.I., Revelli , R. and Ridolfi , L. 2014. Hyporheic flow and transport processes: mechanisms, models, and biogeochemical implications. Reviews of Geophysics 52, 603 - 679.

Bottacin-Busolin, A., Singer, A., Zaramella, M., Battin, T.J. and Marion, A. 2009. Effects of Streambed Morphology and Biofilm Growth on the Transient Storage of Solutes. Environmental Science Technology 43, 73337-77342.

Boulton, A.J., Findlay, S., Marmonier, P., Stanley, E.H., Valett, H.M., 1998.The functional significance of the hyporheic zone in streams and rivers. Annual Review of Ecology and Systematics 29: 59-81.

Boulton, A.J. 2007. Hyporheic rehabilitation in rivers: restoring vertical connectivity. Freshwater Biology 52, 632-650.

Cai, X., Yao, L., Sheng, Q., Jiang, L., Dahlgren, R.A., Wang,T., 2018. Properties of bacterial communities attached to artificial substrates in a hypereutrophic urban river. AMB Express 8: PMC5815975

Cardenas, B.M., Wilson, J.L. and Haggerty, R. 2008. Residence time of bedform-driven hyporheic exchange. Advances in Water Resources 31, 1382-1386.

Caruso, A., Boano, F., Ridolfi, L., Chopp, D.L. and Packman, A. 2017. Biofilm-induced bioclogging produces sharp interfaces in hyporheic flow, redox conditions, and microbial community structure. Geophysical Research Letters 44, 4917–4925.

Chen, X.D., Zhang, C.K., Zhou, Z., Gong, Z., Zhou, J.J., Tao, J.F., Paterson, D.M. and Feng, Q. 2017. Stabilizing Effects of Bacterial Biofilms: EPS Penetration and Redistribution of Bed Stability Down the Sediment Profile. 122(12), 3113-3125.

Clark, J.J., Qian, Q., Voller, V.R. and Stefan, H.G. 2018. Hyporheic exchange in a gravel bed flume with and without traveling surface waves. Advances in Water Research Volume 123, 120-133.

Danczak, R.E., Sawyer, A.H., Williams, K.H., Stegen, J.C., Hobson, C. and Wilkins, M.J. 2016. Seasonal hyporheic dynamics control coupled microbiology and geochemistry in Colorado River sediments. Journal of Geophysical Research: Biogeosciences 121(12), 2976-2987.

Dubois, M., Gilles, K.A., Hamilton, J.K., Rebers, P.A., Smith, F., 1956. Colorimetric method for determination of sugars and related substances. Anal. Chem. 28, 350–356.

Elliott, A.H. and Brooks, N.H. 1997. Transfer of Nonsorbing Solutes to a Streambed with Bed Forms: Theory. Water Resources Research 33, 123-136.

Fischer, C.R., Klein-Marcuschamer, D. and Stephanopoulos, G. 2008. Selection and optimization of microbial hosts for biofuels production. Metabolic engineering 10, 295-304.

Gandy, C.J., Smith, J.W.N. and Jarvis, A.P. 2007. Attenuation of mining-derived pollutants in the hyporheic zone: A review. Science of the Total Environment 373, 435-446.

Gibert, J.,J. A. Stanford, M. J. Dole-Oliver, and J. V. Ward (1994), Basic attributes of groundwater ecosystems and prospects for research, in *Groundwater Ecology*, edited by J. Gilbert, D. L. Danielpol, and J. A. Standford, pp. 8–40, Elsevier, New York.

Gomez-Velez, J.D., Wilson, J.L., Cardenas, M.B. and Harvey, J.W. 2017. Flow and Residence Times of Dynamic River Bank Storage and Sinuosity-Driven Hyporheic Exchange. Water Resources Research 53(10), 8572-8595.

Haggerty, R., Ribot, M., Singer, G.A., Martí, E., Argerich, A., Agell, G. and Battin, T.J. 2014. Ecosystem respiration increases with biofilm growth and bed forms: Flume measurements with resazurin. Journal of Geophysical Research: Biogeosciences 119(12), 2220-2230.

Hall-Stoodley, L. and Stoodley, P. 2002. Developmental regulation of microbial biofilms. . Current Opinion in Biotechnology 13, 228–233.

Hancock, P.J. 2002. Human Impacts on the Stream–Groundwater Exchange Zone. Environmental Management 29, 763–781.

Harvey, J., Gomez-Velez, J., Schmadel, N., Scott, D., Boyer, E., Alexander, R., Eng, K., Golden, H., Kettner, A., Konrad, C., Moore, R., Pizzuto, J., Schwarz, G., Soulsby, C. and Choi, J. 2019. How Hydrologic Connectivity Regulates Water Quality in River Corridors. JAWRA Journal of the American Water Resources Association 55(2), 369-381.

Harvey, J., Gomez-Velez, J., Schmadel, N., Scott, D., Boyer, E., Alexander, R., Eng, K., Golden, H., Kettner, A., Konrad, C., Moore, R., Pizzuto, J., Schwarz, G., Soulsby, C. and Choi, J. 2019. How Hydrologic Connectivity Regulates Water Quality in River Corridors. JAWRA Journal of the American Water Resources Association 55(2), 369-381.

Harvey , J.W. and Wagner, B.J. 2002. Streams and Ground Waters, pp. 3-44, Academic Press, San Diego

Hester, E.T. and Doyle, M.W. 2008. In-stream geomorphic structures as drivers of hyporheic exchange. Water Resources Research 44, W03417, doi:10.1029/2006WR005810.

Jarvie, H.P., Jürgens, M.D., Williams, R.J., Neal, C., Davies, J.J.L., Barrett, C. and White, J. 2005. Role of river bed sediments as sources and sinks of phosphorus across two major eutrophic UK river basins: the Hampshire Avon and Herefordshire Wye. Journal of Hydrology 304(1), 51-74.

Jones, J.B. and Mulholland , P.J. 2000. Streams and Ground Waters, Academic Press, San Diego.

Julien, B., Kaiser, A.D. and Garza, A. 2000. Spatial control of cell differentiation in Myxococcus xanthus. Proceedings of the National Academy of Sciences 97(16), 9098.

Kowalczyk, A., Price, O.R., van der Gast, C.J., Finnegan, C.J., van Egmond, R.A., Schafer, H. and Bending, G.D. 2016. Spatial and temporal variability in the potential of river water biofilms to degrade p-nitrophenol. Chemosphere 164, 355-362.

Krause, S., Tecklenburg, C., Munz, M. and Naden, E. 2013. Streambed nitrogen cycling beyond the hyporheic zone: flow controls on horizontal patterns and depth distribution of nitrate and dissolved oxygen in the upwelling groundwater of a low- land river. Journal of Geophysical Research: Bioegeosciences 118, 54–67.

Larned, S.T., Packman , A.I., Plew , D.R. and Vopel, K. 2011. Interactions between the mat-forming alga D*idymosphenia geminataa*nd its hydrodynamic environment. Limnology and Oceanography 1, 4-22.

Lautz, L.K., Siegel, D.I. and Bauer, R.L. 2006. Impact of debris dams on hyporheic interaction along a semi-arid stream. Hydrological Processes 20(1), 183-196.

Lewandowski, J., Arnon, S., Banks, E., Batelaan, O., Betterle, A., Broecker, T., Coll, C., Drummond, J.D., Gaona Garcia, J., Galloway, J., Gomez-Velez, J., Grabowski, R.C., Herzog, S.P., Hinkelmann, R., Höhne, A., Hollender, J., Horn, M.A., Jaeger, A., Krause, S., Löchner Prats, A., Magliozzi, C., Meinikmann, K., Mojarrad, B.B., Mueller, B.M., Peralta-Maraver, I., Popp, A.L., Posselt, M., Putschew, A., Radke, M., Raza, M., Riml, J., Robertson, A., Rutere, C., Schaper, J.L., Schirmer, M., Schulz, H., Shanafield, M., Singh, T., Ward, A.S., Wolke, P., Wörman, A. and Wu, L. 2019. Is the Hyporheic Zone Relevant beyond the Scientific Community? Water 11(11), 2230.

Li, Z., Che, J., Xue, J., Wang, G., Yu, E., Xia, Y., Yu, D., Zhang, K. 2007. Microbial succession in biofilms growing on artificial substratum in subtropical freshwater aquaculture ponds. FEMS Microbiology Letters 364, https://doi.org/10.1093/femsle/fnx017

Liu, X., Lv, K., Deng, C., Yu, Z., Shi, J. and Johnson, A.C. 2019. Persistence and migration of tetracycline, sulfonamide, fluoroquinolone, and macrolide antibiotics in streams using a simulated hydrodynamic system. Environmental Pollution 252, 1532-1538.

Magliozzi, C., Gianpaolo, C., Grabowsk, R.C., Packman, A.I. and Krause, S. 2019. A multiscale statistical method to identify potential areas of hyporheic exchange for river restoration planning. Science of the Total Environment 111, 311-323.

Magliozzi, C., Grabowski, R.C., Packman, A.I. and Krause, S. 2018. Toward a conceptual framework of hyporheic exchange across spatial scales. Hydrology and Earth System Sciences 22, 6163–6185.

Marion, A., Bellinello, M., Guymer, I. and Packman, A. 2002. Effect of Bed Form Geometry on the Penetration of Nonreactive Solutes into a Streambed. Water Resources Research 38, 27-21—27-12.

Nash, J.E., Sutcliffe, J.V., 1970. River flow forecasting through conceptual models part I-discussion of principles. Journal of Hydology 10, 282e290.

Nogaro G., Datry T., Mermillod-Blondin F., Descloux S. & Montuelle B. 2010. Influence of streambed sediment clogging on microbial processes of the hyporheic zone. Freshwater Biology, 55, 1288– 1302.

Nogaro, G., Datry , T., Mermillod-Blondin , F., Foulquier, A. and Montuelle, B. 2013. Influence of hyporheic zone characteristics on the structure and activity of microbial assemblages. Freshwater Biology (58), 2567 – 2583.

O'Connor, B.L. and Harvey, J.W. 2008. Scaling hyporheic exchange and its influence on biogeochemical reactions in aquatic ecosystems. Water Resources Research 44(12).

Ogink, H.J.M. 1988 Hydraulic roughness of bedforms, Delft, Netherlands.

Orr, C.H., Clark , J.J., Wilcock , P.R., Finlay , J.C. and Doyle, M.W. 2009. Comparison of morphological and biological control of exchange with transient storage zones in a field-scale flume. Journal of Geophysical Research 114, G02019.

Paarlberg, A.J., Dohmen-Janssen, C.M., Hulscher, S.J.M.H. and Termes, P. 2009. Modeling river dune evolution using a parameterization of flow separation. Journal of Geophysical Research: Earth Surface 114(F1).

Packman, A.I., Brooks, N.H. and Morgan, J.J. 2002. A physicochemical model for colloid exchange between a stream and a sand streambed with bed forms. Water Resources Research 36, 2351-2361.

Parker, S.P., Bowden, W.B., Flinn, M.B., Giles, C.D., Arndt, K.A., Beneš, J.P. and Jent, D.G. 2018. Effect of particle size and heterogeneity on sediment biofilm metabolism and nutrient uptake scaled using two approaches. 9(3), e02137.

Peralta-Maraver, I., Reiss, J. and Robertson, A.L. 2018. Interplay of hydrology, community ecology and pollutant attenuation in the hyporheic zone. Science of The Total Environment 610-611, 267-275.

Peter, K.T., Herzog, S., Tian, Z., Wu, C., McCray, J.E., Lynch, K. and Kolodziej, E.P. 2019. Evaluating emerging organic contaminant removal in an engineered hyporheic zone using high resolution mass spectrometry. Water Research 150, 140-152.

Richardson, C.P. and Parr, A.D. 1988. Modified Fickian model for solute uptake by runoff. Journal of Environmental Engineering 114, 792-809.

Sabater, F. and Vila, P.B. 1991. The hyporheic zone considered as an ecotone. Oecologia Aquatica, 10, 35±43.

Sawyer, A.H., Cardenas, M.B., Bomar, A. and Mackey, M. 2009. Impact of dam operations on hyporheic exchange in the riparian zone of a regulated river. Hydrological Processes 23, 2129-2137.

Schaper, J., Posselt, M., McCallum, J., Banks, E., Hoehne, A., Meinikmann, K., Shanafield, M., Batelaan, O. and Lewandowski, J. 2018. Hyporheic Exchange Controls Fate of Trace Organic Compounds in an Urban Stream. Environmental Science and Technology 52, 12285–12294.

Schaper, J.L., Posselt, M., Bouchez, C., Jaeger, A., Nuetzmann, G., Putschew, A., Singer, G. and Lewandowski, J. 2019. Fate of Trace Organic Compounds in the Hyporheic Zone: Influence of Retardation, the Benthic Biolayer, and Organic Carbon. Environmental Science & Technology 53(8), 4224-4234.

Scheidweiler, D., Peter, H., Pramateftaki, P., de Anna, P., Battin, T.J., 2019. Unravelling the biophysical underpinnings to the success of multispecies biofilms in porous environments. The ISME Journal 13**,** 1700–1710.

Sekar, V.P. Venugopalan, K. Nandakumar, K.V.K. Nair, V.N.R., 2004. RaoEarly stages of biofilm succession in a lentic freshwater environment. Hydrobiologia, 512: 97-108

Stanford, J. A., and J. V. Ward (1993), An ecosystem perspective of alluvial rivers: Connectivity and the hyporheic corridor, Journal of the North American Benthological Society 12, 48–60.

Stegen, J.C., Fredrickson , J.K., Wilkins , M.J., Nelson , W.C., Arntzen , E.V., Chrisler , W.B., Chu , R.K., Danczak , R.E., Fansler , S.J., Kennedy , D.W., Resch, C.T. and Tfaily, M. 2016. Groundwater–surface water mixing shifts ecological assembly processes and stimulates organic carbon turnover. Nature Communications 7, 11237.

Tien, C-J., Wu, W-H., Chuang, T-L., Chen, C.S., 2009. Development of river biofilms on artificial substrates and their potential for biomonitoring water quality. Chemosphere 9: 1288-1295.

Tonina , D. and Buffington, J.M. 2007. Hyporheic exchange in gravel bed rivers with pool-riffle morphology; laboratory experiments and three-dimensional modeling. Water Resources Research 43, W01421.

Triska, F.J., Duff, J.H. and Avanzion, R.J. 1993. Patterns of hydrological exchange and nutrient transformation in the hyporheic zone of a gravel-bottom stream: examining terrestrial—aquatic linkages. Freshwater Biology 29, 259-274.

Wijbenga, J.H. 1990 Flow resistance and bed-form dimensions for varying flow conditions. Relation between bed forms and friction in streams., Toegepast Onderzoek Waterstaat.

Williams, D. D., and H. B. N. Hynes. 1974. The occurrence of benthos deep in the substratum of stream, Freshwater Biology, 4, 233–256.

Wimpenny, J., Manz, W. and Szewzyk, U. 2000. Heterogeneity in Biofilms . FEMS Microbiology Reviews 24, 661-671.

Zimmer, M.A. and Lautz, L.K. 2014. Temporal and spatial response of hyporheic zone geochemistry to a storm event. Hydrological Processes 28(4), 2324-2337.

Table 1. Summary of goodness of fit metrics for the models. R^2 values and slope of regression lines between modelled and measured biofilm and hyporheic exchange data for the model approaches, along with Nash-Sutcliffe efficiency (NSE) values. n = number of samples.

	Biomass		**Hyporheic Exchange in all experimental systems**	**Hyporheic Exchange in flat and two-dune 0.5 mm sediment systems**
Significant predictors	*Depth* *Sediment size* *Bedform*	*Days* *Sediment Size* *Bedform*	*Sediment Size* *Bedform* *Biofilm*	*Biofilm*
n	540	198	198	66
R^2	0.68	0.76	0.66	0.54
NSE	0.74	0.90	0.38	0.60

Figure 1.
Figure 2.
Figure 3.
Figure 4.
Figure 5.
Figure 6.
Figure 7.
Figure 8.

Declaration of competing interest

The authors declare that they have no known competing financial interests or personal relationships that could have appeared to influence the work reported in this paper.

Credit Author Statement

Sarah Cook: writing- original draft preparation, data curation, formal analysis, **Oliver Price:** writing – review and editing, supervision, conceptualization, **Andrew King**: investigation, **Chris Finnegan**: writing – review and editing, supervision, **Roger van Egmond**: writing – review and editing, supervision, **Hendrik Schäfer**: writing – review and editing, supervision, **Jonathan M. Pearson**: writing – review and editing, supervision, project administration, funding acquisition, conceptualization, methodology, **Soroush Abolfathi**: formal analysis, writing – review and editing, visualization, **Gary D. Bending**: writing – review and editing, supervision, project administration, funding acquisition, conceptualization, methodology, resources.

Graphical abstract

Highlights

- Interdisciplinary investigation of mechanisms controlling hyporheic exchange.
- Sediment size modifies hyporheic exchange in systems with limited bedform.
- Bedform structures can overcome the biological control over hyporheic exchange.

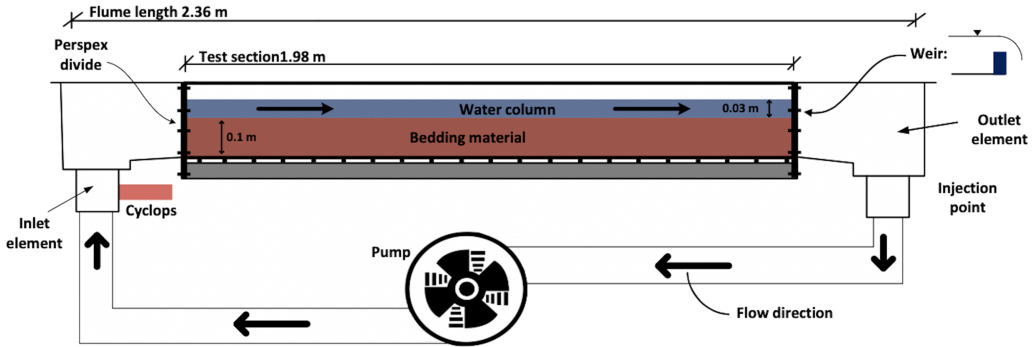
Flume length 2.36 m
Perspex divide
Test section1.98 m
Weir:
Water column
0.03 m
0.1 m
Bedding material
Outlet element
Injection point
Inlet element
Cyclops
Pump
Flow direction

Figure 1

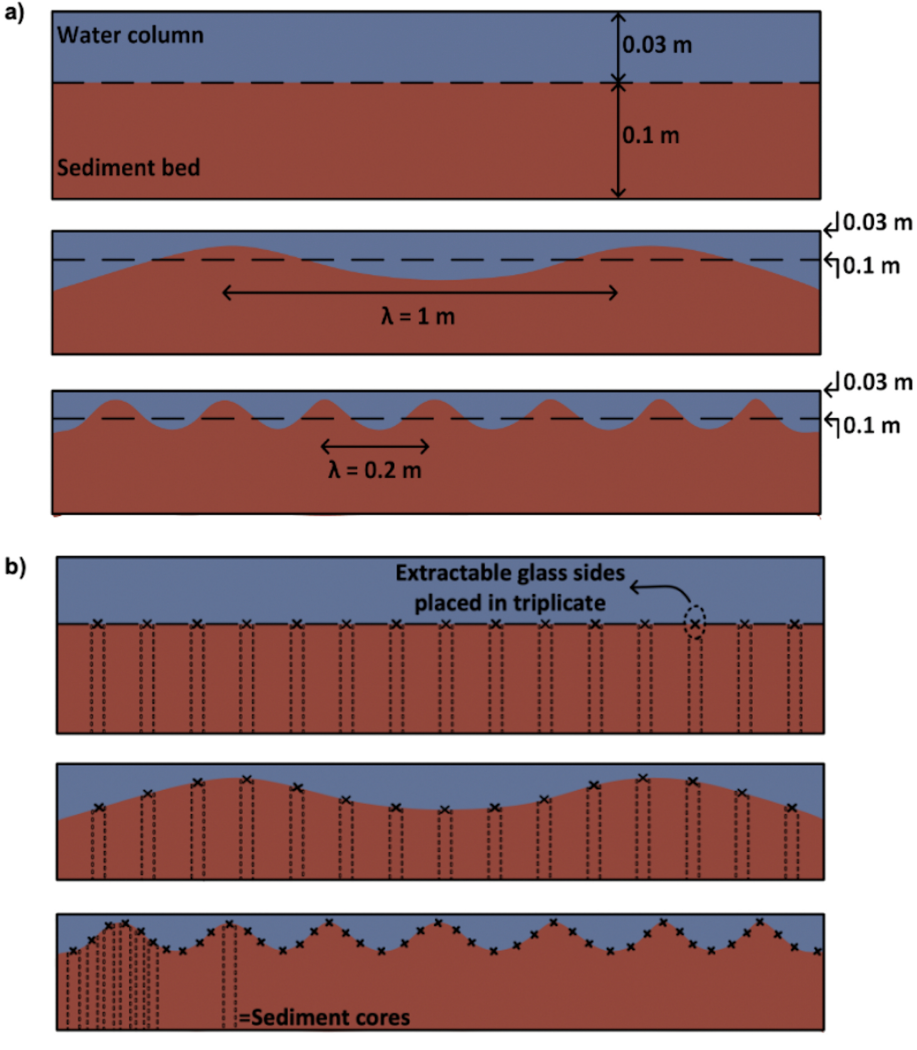
a)
Water column
0.03 m
0.1 m
Sediment bed
0.03 m
0.1 m
λ = 1 m
0.03 m
0.1 m
λ = 0.2 m
b)
Extractable glass sides
placed in triplicate
=Sediment cores

Figure 2

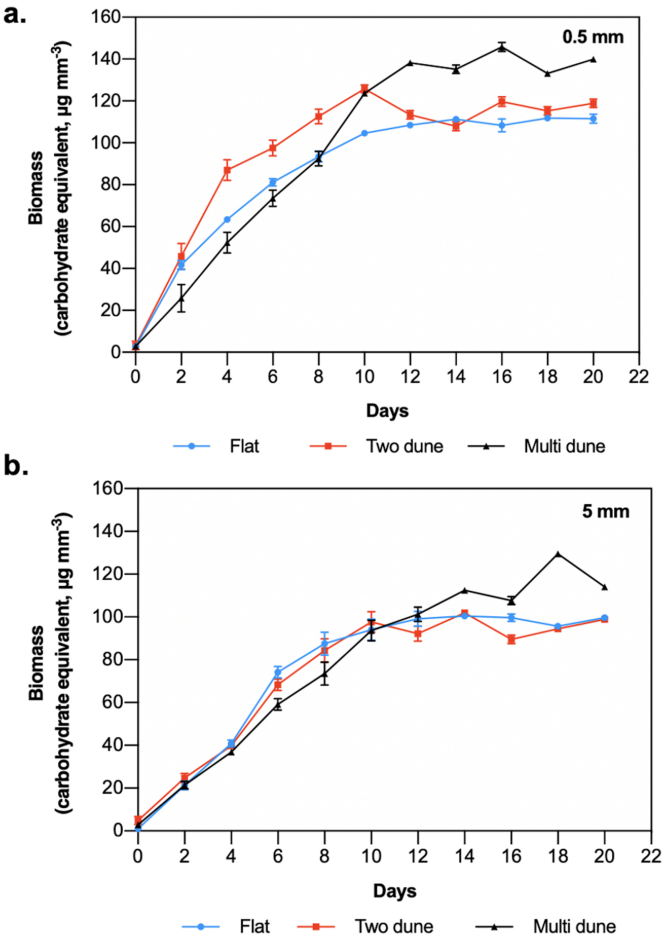
a.
0.5 mm
Biomass
(carbohydrate equivalent, µg mm-3)
Days
Flat
Two dune
Multi dune
b.
5 mm
Biomass
(carbohydrate equivalent, µg mm-3)
Days
Flat
Two dune
Multi dune

Figure 3

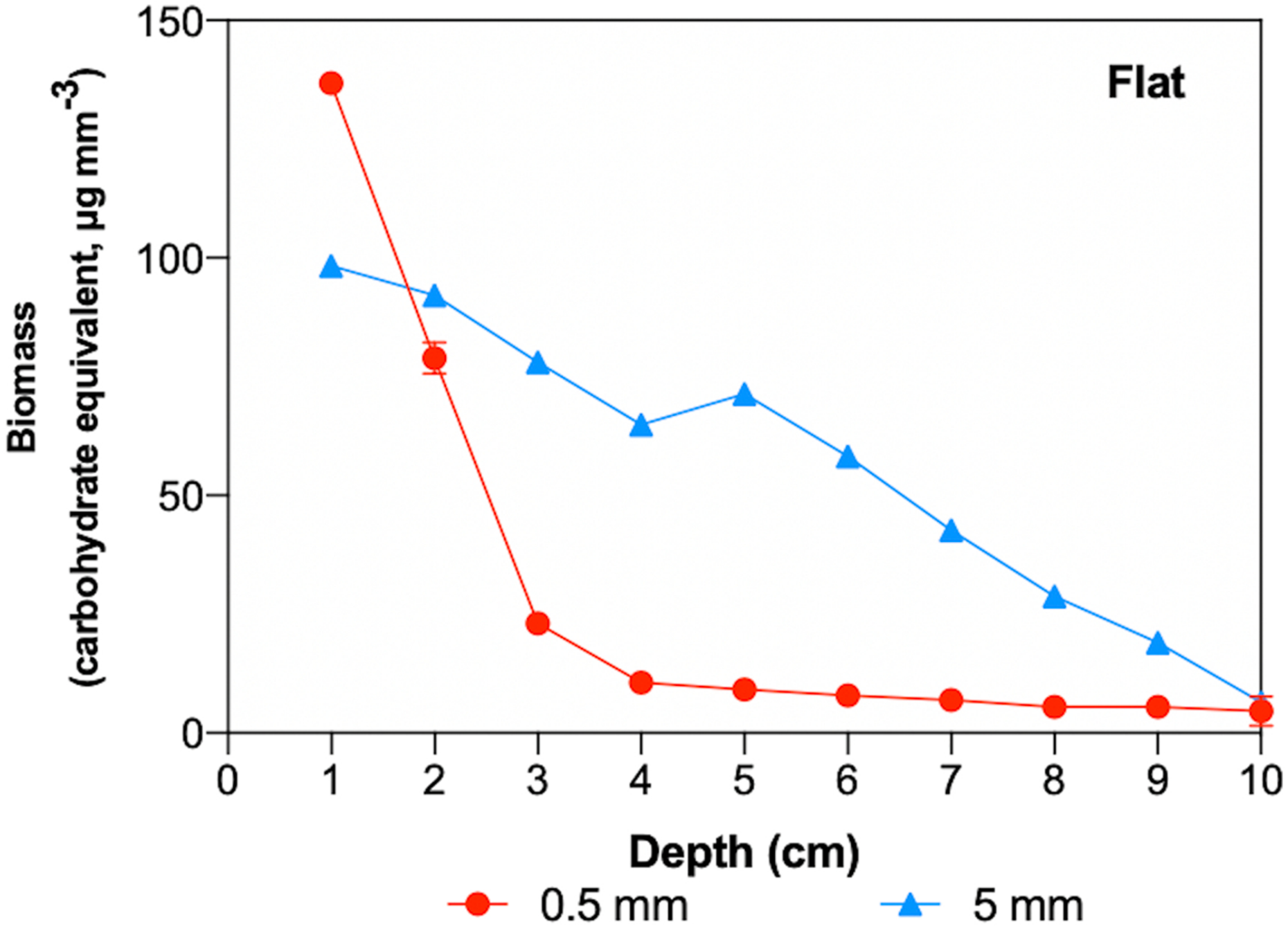
Flat
Biomass
(carbohydrate equivalent, µg mm-3)
150
100
50
0
0
1
2
3
4
5
6
7
8
9
10
Depth (cm)
0.5 mm
5 mm

Figure 4

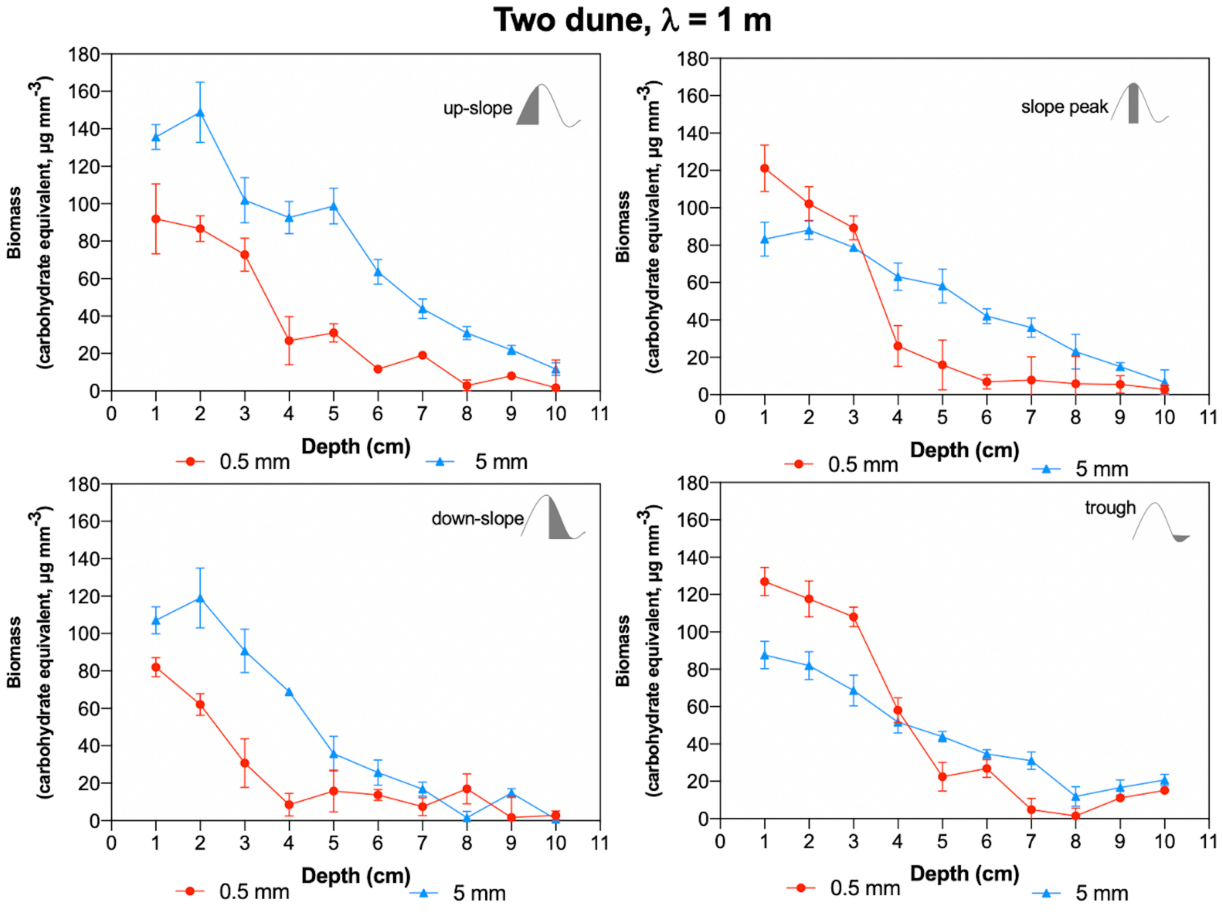
Two dune, λ = 1 m
up-slope
slope peak
down-slope
trough
Biomass
(carbohydrate equivalent, µg mm-3)
Depth (cm)
0.5 mm
5 mm

Figure 5

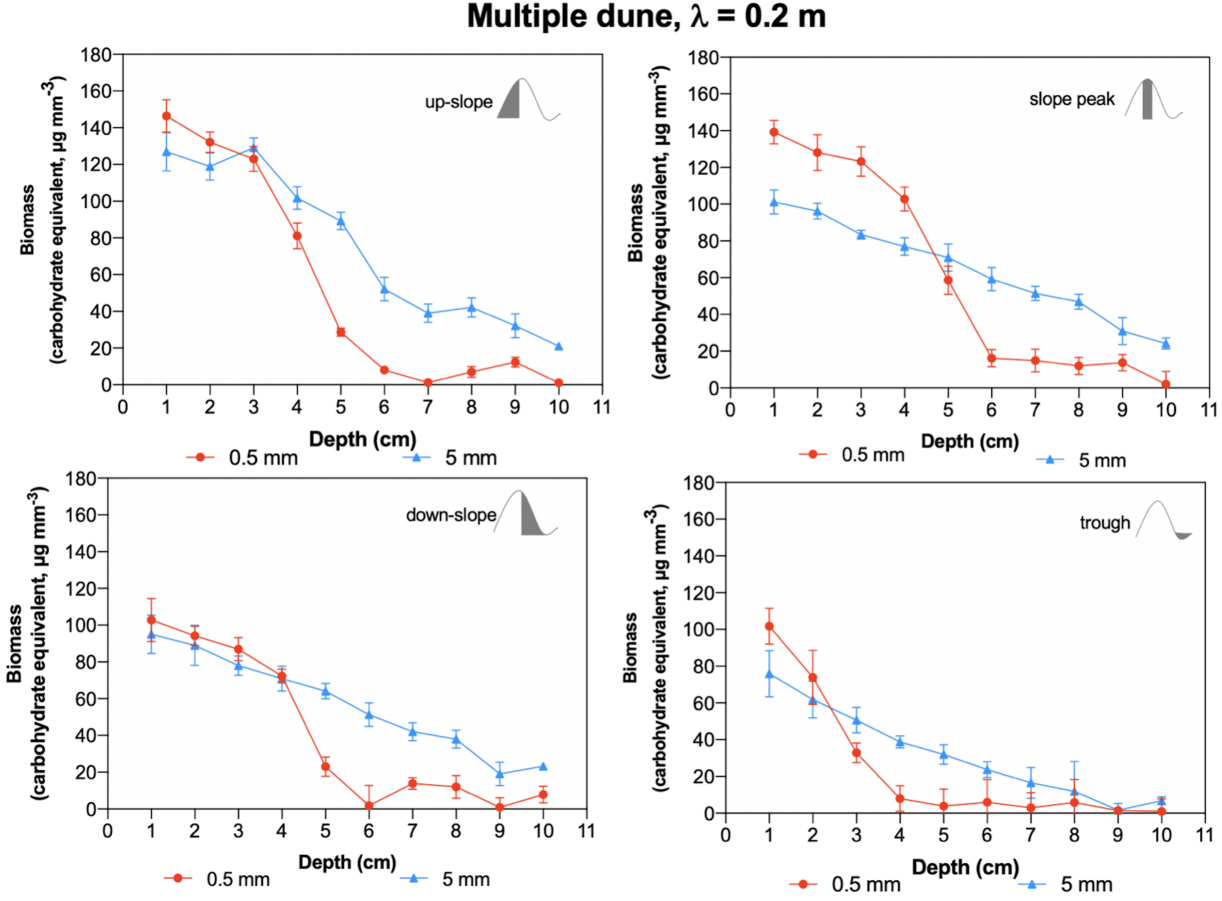
Multiple dune, λ = 0.2 m
up-slope
slope peak
down-slope
trough
Biomass
(carbohydrate equivalent, µg mm-3)
Depth (cm)
0.5 mm
5 mm

Figure 6

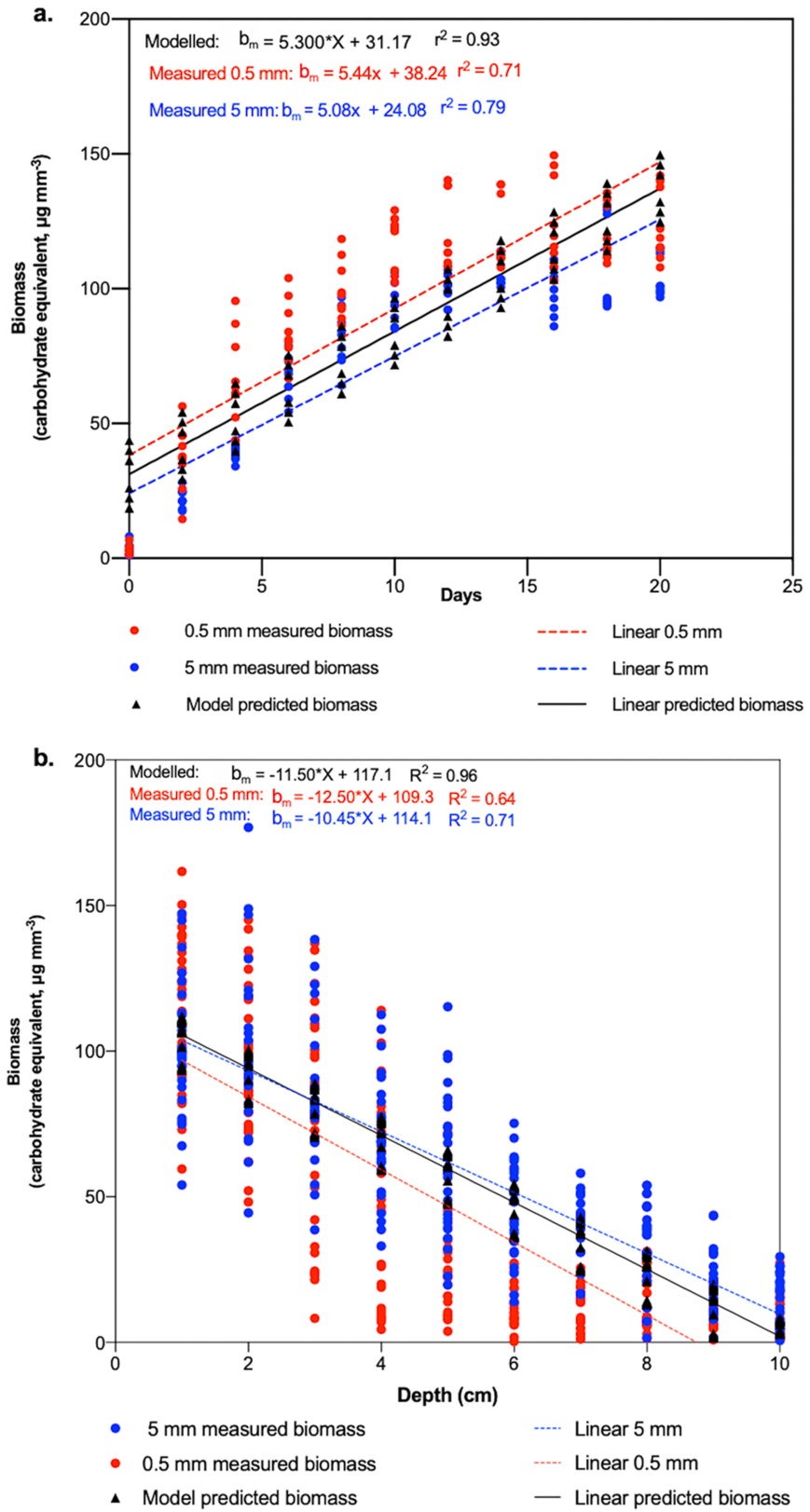
a.
Modelled: b_m = 5.300*X + 31.17 r^2 = 0.93
Measured 0.5 mm: b_m = 5.44x + 38.24 r^2 = 0.71
Measured 5 mm: b_m = 5.08x + 24.08 r^2 = 0.79
Biomass (carbohydrate equivalent, µg mm-3)
Days
0.5 mm measured biomass
5 mm measured biomass
Model predicted biomass
Linear 0.5 mm
Linear 5 mm
Linear predicted biomass
b.
Modelled: b_m = -11.50*X + 117.1 R^2 = 0.96
Measured 0.5 mm: b_m = -12.50*X + 109.3 R^2 = 0.64
Measured 5 mm: b_m = -10.45*X + 114.1 R^2 = 0.71
Biomass (carbohydrate equivalent, µg mm-3)
Depth (cm)
5 mm measured biomass
0.5 mm measured biomass
Model predicted biomass
Linear 5 mm
Linear 0.5 mm
Linear predicted biomass

Figure 7

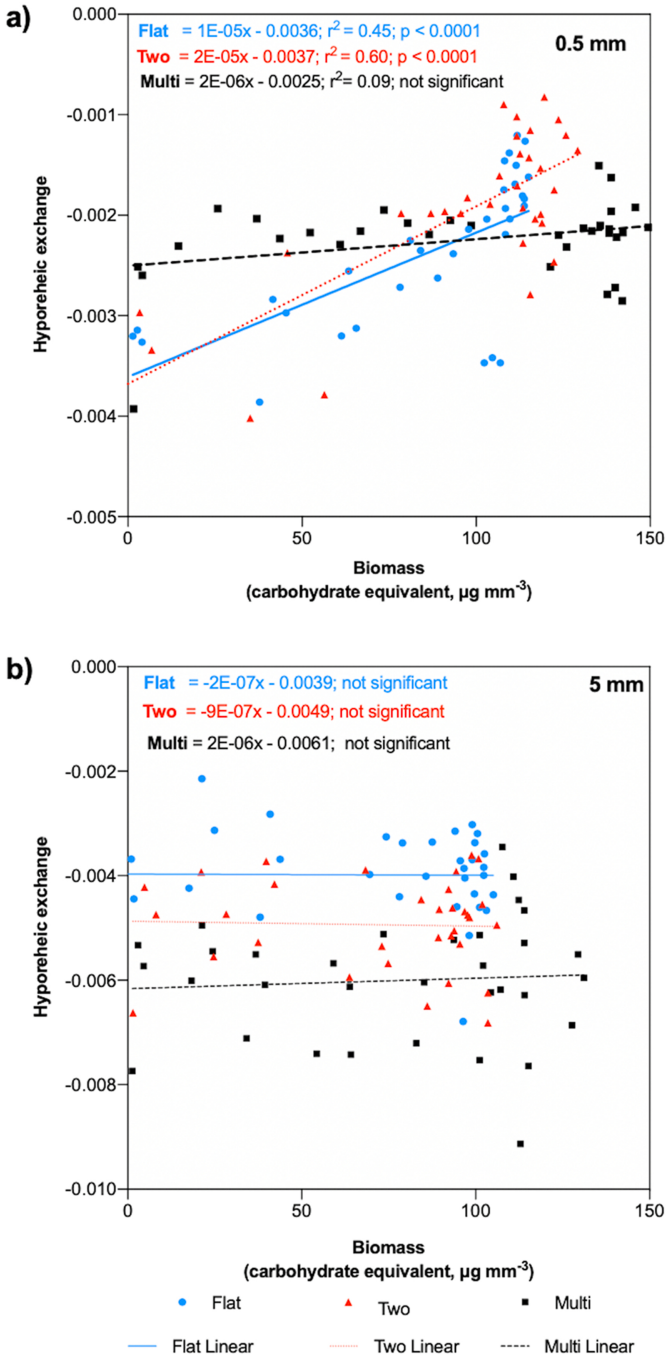
a)
Flat = 1E-05x - 0.0036; r2 = 0.45; p < 0.0001
Two = 2E-05x - 0.0037; r2 = 0.60; p < 0.0001
Multi = 2E-06x - 0.0025; r2= 0.09; not significant
0.5 mm
Hyporeheic exchange
0.000
-0.001
-0.002
-0.003
-0.004
-0.005
0
50
100
150
Biomass
(carbohydrate equivalent, µg mm-3)
b)
Flat = -2E-07x - 0.0039; not significant
Two = -9E-07x - 0.0049; not significant
Multi = 2E-06x - 0.0061; not significant
5 mm
Hyporeheic exchange
0.000
-0.002
-0.004
-0.006
-0.008
-0.010
0
50
100
150
Biomass
(carbohydrate equivalent, µg mm-3)
Flat
Two
Multi
Flat Linear
Two Linear
Multi Linear

Figure 8